Synthesis of $LiCoO_2$ using acrylic acid and its electrochemical properties for Li secondary batteries

Won-Sub Yoon, Kwang-Bum Kim *

Department of Metallurgical Engineering, Yonsei University, 134 Shinchon-dong, Seodaemoon-gu, Seoul, 120-749 South Korea

Abstract

$LiCoO_2$ powders were synthesized by the sol–gel process at various temperatures using acrylic acid as a chelating agent and their structural and electrochemical properties were systematically investigated by X-ray diffraction (XRD), extended X-ray absorption fine structure (EXAFS), Electrochemical voltage spectroscopy (EVS), cyclic voltammetry (CV), and galvanostatic charge/discharge experiments. In this study, the gel-derived $LiCoO_2$ samples calcined at 600°C or above were found to be a well-developed layered high temperature-$LiCoO_2$ (HT-$LiCoO_2$). In the EVS of all the gel-derived HT-$LiCoO_2$ samples, the peak potential separation of 10 mV was observed regardless of the calcination temperature, indicating that these samples have basically the same thermodynamic reversibility for intercalation/deintercalation of Li ions. The change of the main peak potentials and currents in cyclic voltammograms with increasing calcination temperature could be explained by the effect of particle size. © 1999 Elsevier Science S.A. All rights reserved.

Keywords: Sol–gel process; $LiCoO_2$; Lithium rechargeable batteries; EXAFS; EVS

1. Introduction

Lithiated transition metal oxides have been extensively studied as cathode materials for commercial lithium ion rechargeable batteries [1–4]. Among those oxides, $LiCoO_2$ is most widely used as the cathode material of commercial secondary lithium batteries due to its advantages including easy preparation and high theoretical specific capacity [5].

The structure of $LiCoO_2$ materials varies from low temperature (LT) phase to high temperature (HT) phase as calcination temperature increases. HT-$LiCoO_2$ crystallizes in a layer structure isotypic with α-$NaFeO_2$ based on a close-packed network of oxygen atoms with Li^+ and Co^{3+} ions ordering on alternating (111) planes of the cubic rock-salt structure [6,7]. The structure of LT-$LiCoO_2$ shows a partial disordering of Co and Li planes resulting in a different structure from HT-$LiCoO_2$ [8,9]. LT-$LiCoO_2$ and HT-$LiCoO_2$ display different electrochemical properties. For instance, LT-$LiCoO_2$ shows deintercalation/intercalation reactions of Li at lower potentials than HT-$LiCoO_2$.

A synthesis of $LiCoO_2$ is generally divided into two methods; a solid state method and a solution method. A solid state method consists of grinding and calcination of

hydroxides or carbonates such as $LiOH$, Li_2CO_3 and $CoCO_3$. This method has disadvantages such as broader particle size distribution, higher calcination temperature, longer reaction time. A solution method requires condensation of a solid oxide network starting from soluble species and a thermal treatment leading to oxide $LiCoO_2$. This method makes possible a better mixing of the elements and therefore a better reactivity of the mixture, which then allows lower reaction temperature and shorter reaction time. Additionally, the resulting powders also show good stoichiometric control and narrow particle size distribution.

Two preparation techniques have been reported as a solution method for synthesis of $LiCoO_2$. One is a synthesis of $LiCoO_2$ using a precipitation process in aqueous solutions of hydroxide, nitrates, and acetates salts [10–13]. The other is a sol–gel process using organic acid as a chelating agent [14–17]. In the sol–gel process, chelating agents previously reported have shown drawbacks such as fluffiness during calcination and need for pH control during the gel-formation. In this study, acrylic acid has been used as a chelating agent in order to overcome the disadvantages of the reported chelating agents. HT-$LiCoO_2$ can be synthesized at a wide temperature range in the sol–gel process. However, systematic investigation of electrochemical properties of $LiCoO_2$ powders synthesized by the sol–gel process at various temperatures has not been re-

* Corresponding author. Tel.: +82-2-361-2839; Fax: +82-2-312-5375; E-mail: kbkim@bubble.yonsei.ac.kr

ported so far. In this study, $LiCoO_2$ powders were synthesized using acrylic acid as a chelating agent and their structural and electrochemical properties were studied as a function of calcination temperature by X-ray diffraction (XRD), extended X-ray absorption fine structure (EXAFS), electrochemical voltage spectroscopy (EVS), cyclic voltammetry (CV), and galvanostatic charge/discharge experiments.

2. Experimental

A stoichiometric amount of Li and Co acetate salts was dissolved in a distilled water and mixed with an aqueous solution of acrylic acid. The resulting solution was mixed with a magnetic stirrer at 70–80°C for several hours to obtain a clear viscous gel. The gel was dried in a vacuum oven at 100°C for several hours. All the $LiCoO_2$ compounds were ground and calcined at 500–900°C for 10 h after pre-calcining the obtained gel precursor at 450°C for 1 h in air.

The crystal structure of $LiCoO_2$ calcined at various temperatures was characterized by XRD. Powder XRD pattern was recorded using an automated Rigaku powder diffractometer using Cu Kα radiation. EXAFS measurements were performed in transmission mode at beamline 3C1 of Pohang Light Source (PLS) using a Si(111) double-crystal monochromator. The storage ring was operated with an electron energy of 2 GeV and a current between 80 and 120 mA. Calibration was carried out prior to all measurements using the first inflection point of the spectrum of Co foil, i.e., Co K-edge = 7709 eV, as a reference.

Cathode specimens were prepared by mixing the $LiCoO_2$ powders with 10 wt.% acetylene black and 6 wt.% PVDF (poly-vinylidene fluoride) in NMP (*n*-methyl pyrrolidone) solution. The mixture was spread on A1 foil with a thickness of 80 μm and pressed. The composite electrodes were dried under vacuum at 150°C for at least 12 h before use. A three-electrode electrochemical cell was employed for electrochemical measurements in which lithium foil was used for both reference and counter electrodes. The electrolyte used was 1 M $LiClO_4$ in propylene carbonate (PC) solution. CV and EVS measurements were carried out using an EG&G Model 273A potentiostat/galvanostat. In the EVS measurements conducted here, the values of potential step (ΔV) and pre-set minimum current (I_{lim}) were 10 mV and 2 mA/g, respectively. All the electrochemical experiments were carried out at room temperature in a glove box filled with purified argon gas.

3. Results and discussion

$LiCoO_2$ powders were synthesized by a sol–gel process using a chelating agent. Acrylic acid was employed as a chelating agent because acrylic acid was found in this work to have advantages such as less fluffiness during pre-calcination and no need for pH control when forming sol–gel unlike other reported chelating agents [15–17]. It is believed that the carboxylic groups on the acrylic acid could form chemical bonds with metal ions [18]. The choice of pre-calcination temperature for the gel precursor was made on the basis of TG–DTA curve. Fig. 1 shows TG–DTA curve of the gel precursor for $LiCoO_2$ prepared for a molar ratio of acrylic acid to total metal ions of 2. The first weight loss in the temperature range of 30–140°C is associated with the departure of water. The weight loss in the temperature range of 200–400°C corresponds to the combustion of organic constituents in the gel precursor, such as acetates and acrylic acid, which occurs with a large exothermic peak at 389°C in the DTA curve. The acrylic acid not only acted as a chelating agent in making a gel but also provided the combustion heat for calcination in the synthesis of $LiCoO_2$ powders. This facilitates the reaction among the constituent metal ions and the synthesis of $LiCoO_2$ powders at a relatively low external temperature [19].

Scanning electron micrographs (SEM) of the powders calcined at various temperatures for 10 h in air are shown in Fig. 2. As the calcination temperature increased, growth kinetics were favored and thus the agglomerated spherical particles became larger. The presence of loosely agglomerated spherical particles with a submicron particle size was observed from the powders calcined at 600 and 700°C. When the precursor powders were calcined at 800°C, the particle size of the powders was abruptly increased up to 1–2 μm.

Fig. 3 shows XRD patterns for the gel-derived samples calcined at various temperatures for 10 h in air after pre-calcining the obtained gel precursor at 450°C for 1 h. HT-$LiCoO_2$ and LT-$LiCoO_2$ can be seen in XRD patterns. The (006) and (012) peaks and (108) and (110) peaks are well-separated in the patterns of HT-$LiCoO_2$ samples, but overlapped with one another in LT-$LiCoO_2$ [9]. XRD
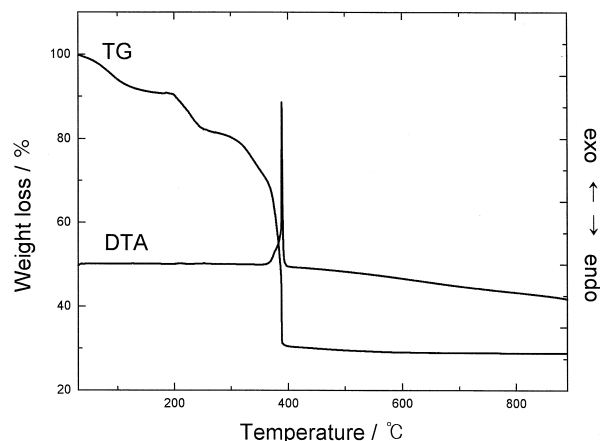

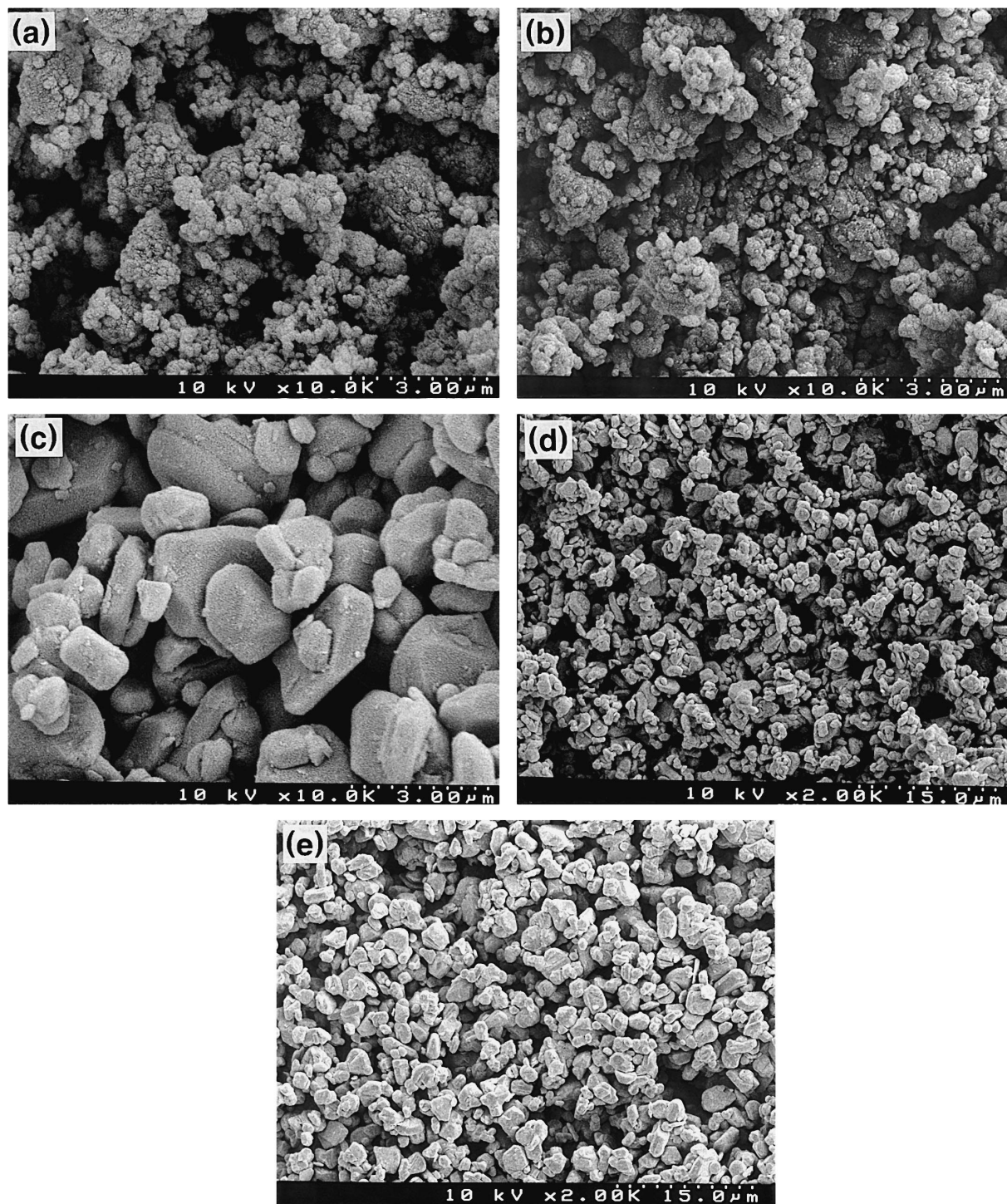Fig. 1. TG and DTA curves of $LiCoO_2$ gel precursor at a heating rate of 2°C/min and an air flow rate of 100 cm^3/min.

Fig. 2. SEM of the LiCoO₂ powders calcined at (a) 600, (b) 700, (c,d) 800 and (e) 900°C; (a), (b), (c): ×10 000 and (d), (e): ×2000.

pattern analysis alone, however, cannot be an absolute measure in distinguishing HT-LiCoO₂ from LT-LiCoO₂ since the analysis is qualitative. Although the XRD patterns for LiCoO₂ samples calcined at 500°C or above show good separations between (006)/(012) and (108)/(110) couples of diffraction lines, they are not sufficient enough to assert that these compounds have a well-developed layered HT-LiCoO₂. Zhecheva et al. [15] reported in their

XRD study that a single-phase HT-LiCoO₂ was synthesized at 400°C for 20 h. However, in step potential electrochemical spectroscopy (SPES), they reported the presence of the reduction peak at ca. 3.5 V, which suggests that it is not a single-phase HT-LiCoO₂. Similarly, Sun et al. [16] reported in their XRD study a synthesis of a single-phase HT-LiCoO₂ at 550°C for 1 h without testing its electrochemical properties.
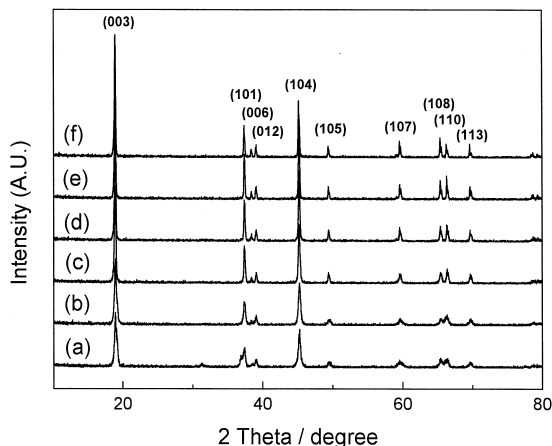
Fig. 3. XRD patterns for the gel-derived materials calcined at various temperatures: (a) 450, (b) 500, (c) 600, (d) 700, (e) 800 and (f) 900°C.

While XRD allows the average long-range structure of a crystalline compound to be determined and described by a unit cell, EXAFS identifies the local structure surrounding a target atom [20]. The Fourier transforms of the cobalt K-edge EXAFS spectra of lithium cobalt oxides are shown in Fig. 4. Normalized EXAFS were converted from energy to k and weighted by k^3 to compensate for attenuation of the amplitude in EXAFS spectra at high k. Fourier transforms were obtained over the range 3.0 to 14.0 Å^{-1}.

A neutron-diffraction study of HT-$LiCoO_2$ by Orman and Wiseman [6] has shown that the layers of lithium and cobalt ions are perfectly ordered; the lithium and cobalt ions occupy 3a and 3b octahedral sites of the trigonal unit cell ($R\bar{3}m$), respectively. In the structure of perfect HT-$LiCoO_2$ A, B, C, and D peaks in Fig. 4 should correspond to six oxygen atoms, six cobalt and six lithium atoms, 12 cobalt and 12 lithium atoms, and 12 cobalt atoms, respectively [13]. Cobalt is the strongest backscatterer in the structure compared to lithium and oxygen. No peak corresponds to lithium atoms in spectrum because lithium is a light element. Since lithium and cobalt cations in LT-$LiCoO_2$ samples are not perfectly ordered in alternate layers, that is, some of the cobalt ions are situated in the lithium layer and some lithium ions in the cobalt layer, the difference in the intensity of the peak for the coordination shell made up only of cobalt atoms results in the difference between HT-$LiCoO_2$ and LT-$LiCoO_2$ [13]. The intensity of D peak of the gel-derived $LiCoO_2$ calcined at 500°C or below decreases as calcination temperature decreases, which indicates that lithium and cobalt cations in $LiCoO_2$ samples obtained at 500°C or below are not perfectly ordered in alternate layers. However, all the gel-derived $LiCoO_2$ samples calcined at 600°C or above have the same intensity of D peak. The results support that these compounds have a well-developed layered HT-$LiCoO_2$ showing good ordering of Li and Co layers.

Fig. 5 shows EVS differential capacity plot for the gel-derived $LiCoO_2$ samples calcined at various tempera-

tures. EVS technique is a powerful method for characterizing the electrochemical properties of alkali metal insertion reactions [21,22]. In the EVS experiment, since cells move on to the next potential step after reaching thermodynamic equilibrium under certain potential step, they are hardly affected by kinetic parameters. Therefore, in the reaction accompanying phase transition, since there are hardly any changes in potential until phase transition is completed, the curve of deferential capacity of potential forms a shape of peak. On the other hand, in the reaction that does not accompany phase transition, a smooth curve is formed. In this experiment, the potential of the $LiCoO_2$ electrode was changed by 10 mV increments and the current was allowed to decay to less than 2 mA/g before the next potential step was applied, which ensured that the electrode was close to thermodynamic equilibrium during the cycling process. In all the gel-derived $LiCoO_2$ electrodes calcined at 600°C or above, the main lithium intercalation and deintercalation peaks appear at the potentials of 3.91 and 3.92 V, respectively, with the same peak potential separation of 10 mV, indicating that these samples have basically the same thermodynamic reversibility for intercalation/deintercalation of Li ions. Two high voltage peaks observed above 4 V may result from phase transition between ordered and disordered lithium ion arrangements in the CoO_2 framework [7]. An irreversible oxidation peak at 3.83 V is shown in the $LiCoO_2$ sample calcined at 500°C, which indicates that the $LiCoO_2$ sample is an intermediate phase between HT-$LiCoO_2$ and LT-$LiCoO_2$.

Fig. 6 presents cyclic voltammograms obtained from the gel-derived $LiCoO_2$ calcined at various temperatures. The cyclic voltammograms were performed at a slow scan rate of 0.01 mV/s. In all the gel-derived $LiCoO_2$ electrodes calcined at 600°C or above, typical cyclic voltammograms of HT-$LiCoO_2$ were observed, which were characterized by three sets of well-defined current peaks [23].
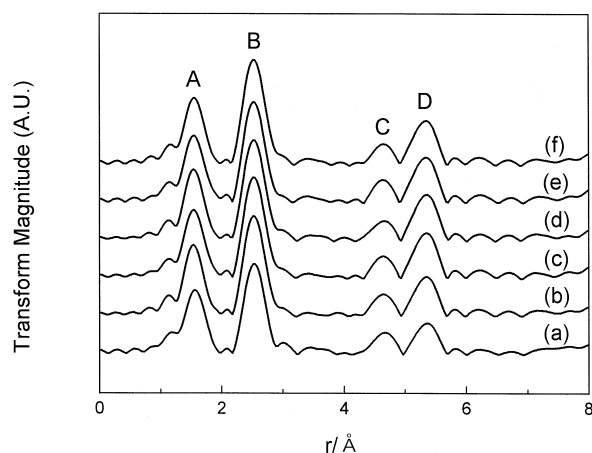

Fig. 4. Fourier transforms of the cobalt K-edge EXAFS spectra of gel-derived materials calcined at various temperatures: (a) 450, (b) 500, (c) 600, (d) 700, (e) 800 and (f) 900°C. The Fourier transforms are not phase-corrected.
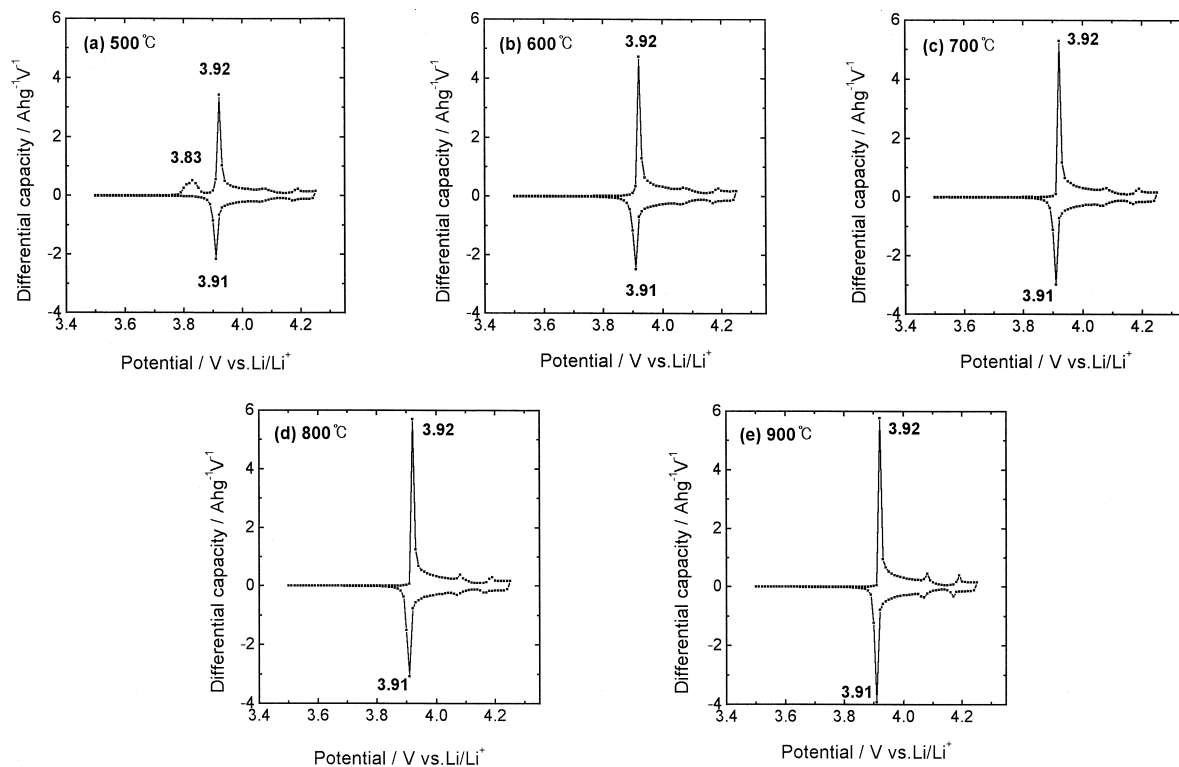
Fig. 5. EVS differential capacity plots for the gel-derived LiCoO$_2$ calcined at various temperatures.
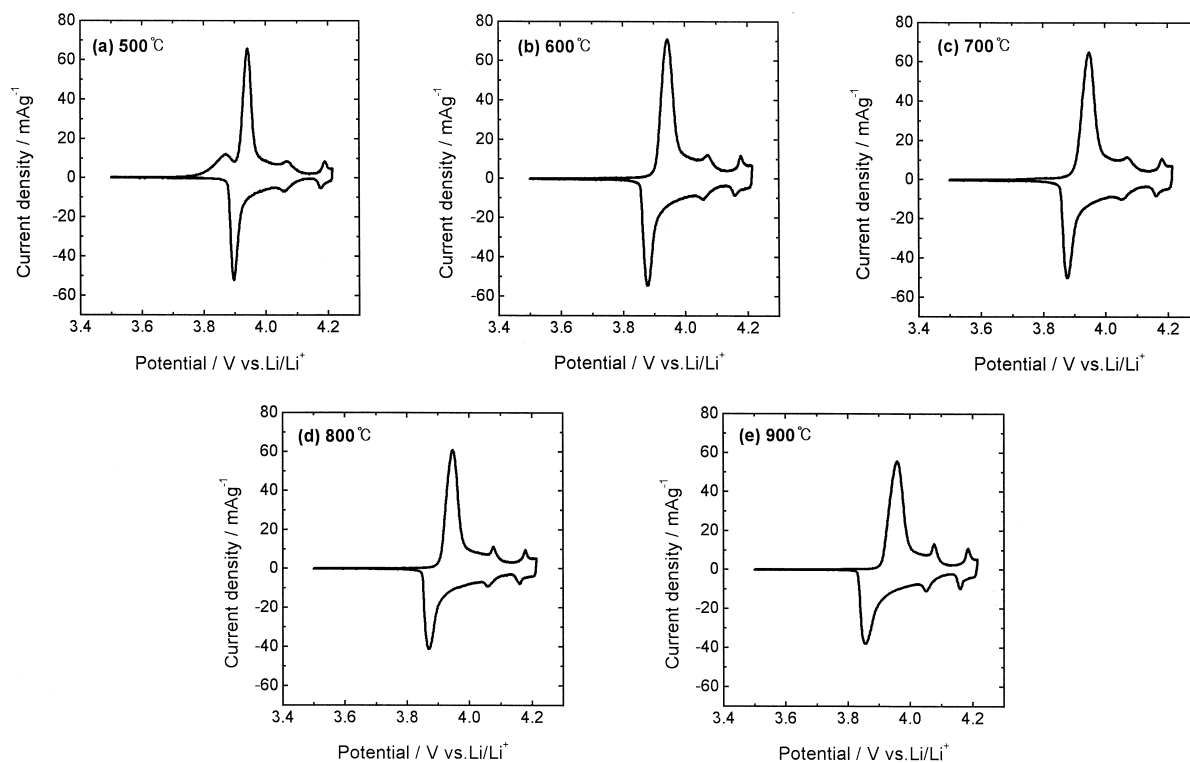
Fig. 6. Cyclic voltammograms obtained from the gel-derived LiCoO$_2$ calcined at various temperatures at a scan rate of 0.01 mV/s.

Although the gel-derived $LiCoO_2$ electrode is a pellet-type electrode containing organic polymer binder, it should be noted that its cyclic voltammogram appeared to be identical to that of binder-free thin film $LiCoO_2$ by Uchida and Saito [23]. This may be ascribed to a slow scan rate of 0.01 mV/s [24] and a homogeneous particle size. The main lithium intercalation and deintercalation peaks appeared at below 4 V. As calcination temperature increased, the peak intensity of the main reduction and oxidation peaks decreased and at the same time, the separation between the reduction and oxidation peak potentials increased. Basically, two reasons are thought to be responsible for the change in the cyclic voltammogram from large to small peak intensity and from narrow to wide peak separation as calcination temperature increases. First, the particle size of $LiCoO_2$ powders prepared at lower temperatures becomes smaller and therefore, the electrodes have larger surface area for reaction, which in turn leads to the increased peak intensity. The particle size of $LiCoO_2$ electrodes prepared at higher temperatures becomes larger and as a result, it takes longer for the lithium ions to diffuse into and from larger particles, which may cause an increased separation of peak potentials [11,25]. Fig. 7 summarizes potential separations between the main reduction and oxidation peaks of CV and EVS for the gel-derived HT-$LiCoO_2$ calcined at various temperatures.

The first charge/discharge behaviors of gel-derived $LiCoO_2$ samples at a constant current rate of $C/5$ are shown in Fig. 8. The cells were first charged from their rest potential up to 4.25 V and then discharged down to 3 V. In the galvanostatic mode, the lithium concentrations, x, were calculated from the elapsed time, the current, and the mass of the active material in the cathode under the assumption that all the current passed was due to lithium insertion or extraction. The gel-derived $LiCoO_2$ electrode calcined at 600°C shows the typical charge/discharge curve of HT-$LiCoO_2$. The charge/discharge curve of HT-
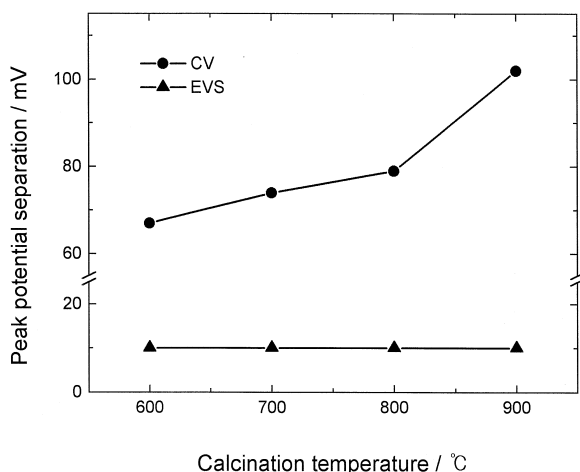

Fig. 7. Separations between the reduction and oxidation peaks for the gel-derived HT-$LiCoO_2$ calcined at various temperatures.
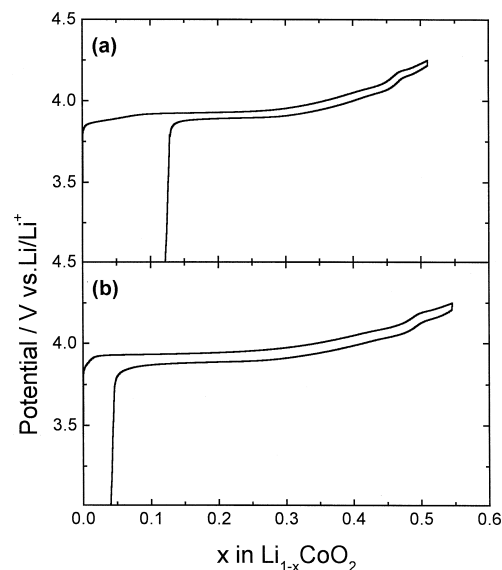

Fig. 8. First charge/discharge curves of gel-derived $LiCoO_2$ calcined at (a) 500 and (b) 600°C at a rate of $C/5$.

$LiCoO_2$ displays a wide potential plateau near 3.9 V. Two smaller plateaus are also present at higher potentials. The occurrence of the wide plateau near 3.9 V is due to the coexistence of two pseudo-phases of an Li-dilute α-phase and an Li-concentrated β-phase [26]. Two smaller plateaus correspond to the order/disorder phase transition arising at around $x = 0.5$ in the HT-$Li_{1-x}CoO_2$ [7]. In the charge curve of the $LiCoO_2$ electrode obtained at 500°C, the curve in the range of $x = 0$–0.1 corresponds to the irreversible oxidation peak in EVS and CV (Figs. 5 and 6), which results in initial capacity loss.

4. Conclusions

$LiCoO_2$ powders were synthesized by the sol–gel process using acrylic acid as a chelating agent. Acrylic acid not only acted as a chelating agent in making a gel but also provided the combustion heat for calcination in the synthesis of $LiCoO_2$ powders, which could lower the calcination temperature at which a single-phase HT-$LiCoO_2$ can be synthesized. XRD and EXAFS results showed that the gel-derived $LiCoO_2$ samples calcined at 600°C or above were a well-developed layered HT-$LiCoO_2$. The electrochemical experiments also showed that the $LiCoO_2$ samples calcined at 600°C or above have the electrochemical properties of HT-$LiCoO_2$. EVS of the gel-derived HT-$LiCoO_2$ showed no change of potential separation in the main oxidation and reduction peaks with calcination temperature, which indicates that these samples have basically the same thermodynamic reversibility for intercalation/deintercalation of Li ions. In their cyclic voltammograms, however, the main peak potential separation increased as calcination temperature increased, which could be explained by the effect of particle size.

Acknowledgements

References

[1] K. Mizushima, P.C. Jones, P.C. Wiseman, J.B. Goodenough, Mater. Res. Bull. 15 (1980) 783.
[2] K. Ozawa, Solid State Ionics 69 (1994) 212.
[3] Yamada, K. Miura, K. Hinokuma, M. Tanaka, J. Electrochem. Soc. 142 (1995) 2149.
[4] T. Ohzuku, M. Kitagawa, T. Hirai, J. Electrochem. Soc. 137 (1990) 769.
[5] T. Nagaura, K. Tozawa, Prog. Batt. Sol. Cells 9 (1991) 209.
[6] H.J. Orman, P.J. Wiseman, Acta Cryst. C40 (1984) 12.
[7] J.N. Reimiers, J.R. Dahn, J. Electrochem. Soc. 139 (1992) 2091.
[8] E. Rossen, J.N. Reimers, J.R. Dahn, Solid State Ionics 62 (1993) 53.
[9] R.J. Gummow, M.M. Thackeray, W.I.F. David, S. Hull, Mater. Res. Bull. 27 (1992) 327.
[10] P. Barboux, J.M. Tarascon, F.K. Shokoohi, J. Solid State Chem. 94 (1991) 185.
[11] R. Yazami, N. Lebrun, M. Bonneau, M. Molteni, J. Power Sources 54 (1995) 389.
[12] B. Garcia, J. Farcy, J.P. Pereira-Ramos, J. Perichon, N. Baffier, J. Power Sources 54 (1995) 373.
[13] B. Garcia, P. Barboux, F. Robot, A. Kahn-Harai, L. Mazerolles, N. Baffier, Solid State Ionics 80 (1995) 111.
[14] M. Yoshio, H. Tanaka, K. Tominaga, H. Noguchi, J. Power Sources 40 (1992) 347.
[15] E. Zhecheva, R. Stoyanova, M. Gorova, R. Alcantara, J. Morales, J.L. Tirado, Chem. Mater. 8 (1996) 1429.
[16] Y.K. Sun, I.H. Oh, S.A. Hong, J. Mater. Sci. 31 (1996) 3617.
[17] I.H. Oh, S.A. Hong, Y.K. Sun, J. Mater. Sci. 32 (1997) 3177.
[18] P.A. Lessing, Ceram. Bull. 68 (1989) 1002.
[19] S. Kumar Saha, A. Pathak, P. Pramanik, J. Mater. Sci. Lett. 14 (1995) 35.
[20] D.C. Koningsberger, R. Prins (Eds.), X-ray Absorption: Principles, Applications, Techniques of EXAFS, SEXAFS, and XANES, Wiley, New York, 1988.
[21] J. Barker, Electrochim. Acta 40 (1995) 1603.
[22] J. Barker, R. Pynenburg, R. Koksbang, J. Power Sources 52 (1994) 185.
[23] I. Uchida, H. Saito, J. Electrochem. Soc. 142 (1995) L139.
[24] M. Broussely, F. Perton, J. Labat, R.J. Staniewicz, A. Romero, J. Power Sources 43 (1993) 209.
[25] I. Uchida, H. Fujiyoshi, S. Waki, J. Power Sources 68 (1997) 139.
[26] Y.M. Choi, S.I. Pyun, J.S. Bae, S.I. Moon, J. Power Sources 56 (1995) 25.